

Method for measurement of diffusivity: Calorimetric studies of Fe/Ni multilayer thin films

Jiaxing Liu and Katayun Barmak*

Department of Applied Physics and Applied Mathematics, Columbia University, New York, NY 10027, USA

Received 8 December 2014; revised 20 February 2015; accepted 21 February 2015

Available online 15 April 2015

A calorimetric method for the measurement of diffusivity in thin film multilayers is introduced and applied to the Fe–Ni system. Using this method, the diffusivity in [Fe (25 nm)/Ni (25 nm)]₂₀ multilayer thin films is measured as $4 \times 10^{-3} \exp(-1.6 \pm 0.1 \text{ eV}/k_B T) \text{ cm}^2/\text{s}$, respectively. The diffusion mechanism in the multilayers and its relevance to laboratory synthesis of L1₀ ordered FeNi are discussed.
 © 2015 Acta Materialia Inc. Published by Elsevier Ltd. All rights reserved.

Keywords: Differential scanning calorimetry; Diffusion; Fe–Ni; Thin films

L1₀ ordered FeNi has recently attracted a great deal of interest on account of its uniaxial magnetic anisotropy of order 10^7 erg/cm^3 and an estimated room-temperature maximum energy product of 40 MGOe [1–3]. Experimental evidence also points to a 100× better elevated temperature stability of intrinsic coercivity compared to the NdFeB magnets [3]. These attractive magnetic properties, along with the relative abundance and ready availability of Fe and Ni, make L1₀ FeNi a very promising candidate as a rare-earth free permanent magnet.

The formation of L1₀ FeNi from a chemically-disordered fcc (A1) matrix requires annealing at temperatures below the order–disorder temperature of 320 °C [4]. However, at these temperatures diffusion is extremely slow. For example, it was calculated that at 300 °C Ni would make only one atomic jump in 10⁴ years [5]. Therefore, it is critical to enhance the low temperature diffusivity in the Fe–Ni system in order to synthesize L1₀ FeNi at laboratory time scales. One approach to enhancing the low temperature diffusivity is bombardment by energetic particles. High-energy neutron and electron bombardment have been shown to be successful in creating additional vacancies, thereby enhancing diffusion and allowing formation of L1₀ FeNi [4,6]. Another approach to diffusion enhancement is the use of ultrafine-grained materials since diffusivity in these materials can be several orders of magnitude higher than bulk diffusivity. This second approach underlies the formation of L1₀ FeNi in Invar alloys that were quenched to form martensite, which upon annealing formed nanometric FeNi grains by recrystallization [7]. A class of materials that is known to be ultrafine-grained is vacuum-deposited thin films, and

therefore the formation of L1₀ FeNi should be possible in such films. This possibility can be evaluated by the measurement of diffusivities in thin film diffusion couples.

Atom migration in a diffusion couple brings about a change in the concentration profile, which can be studied using measurement techniques such as X-ray reflectivity [8], X-ray diffraction (XRD) [9], Auger electron spectroscopy [10], and analytical electron microscopy [11]. The measured change in the concentration profile is then used to determine the diffusion coefficient. Atom migration also results in the release or absorption of heat depending on the sign of the enthalpy of mixing. However, there have been very few reports of measurement of diffusivities using the corresponding heat flow signal. Vohra et al. [12] show that differential scanning calorimetry (DSC), an instrument for measurement of the rate of enthalpy change, can be readily utilized for the study of interdiffusion in multilayer films. However, the method they proposed requires significant device microfabrication and extensive numerical simulation for thermal modeling. In the work presented here, it is shown that the interdiffusion in multilayer thin films can be studied with a simple experimental and calculation procedure using conventional DSC [13].

Isothermal annealing and annealing at a constant heating-rate are two common modes used in DSC experiments. The latter has better signal-to-noise ratio than the former, thus, it is used here for the analysis of diffusion in multilayer films. In this mode, the temperature, T , at time t follows $dT/dt = \beta$, where β is the heating rate.

The solution to the diffusion equation for the concentration, c , as a function of distance, x , at temperature T for a periodic multilayer thin film subjected to annealing at a constant heating-rate is

* Corresponding author; e-mail: kb2612@columbia.edu

$$c(x, T) = \sum_n \left(A_n \sin \frac{2\pi n}{L} x + B_n \cos \frac{2\pi n}{L} x \right) \exp \left(-\frac{4\pi^2 n^2}{L^2} \frac{1}{\beta} \int_0^T D(T') dT' \right) \quad (1)$$

where L is the periodicity of the multilayer structure (i.e., sum of the elemental layer thicknesses), A_n and B_n are constants that are determined by the initial conditions, and D is the diffusivity and follows the Arrhenius ansatz

$$D = D_0 \exp \left(-\frac{E}{k_B T} \right) \quad (2)$$

where D_0 is the pre-exponential term and E is the activation barrier for diffusion.

The heat flow, Q , measured by the DSC, is the result of the enthalpy of mixing H , which itself changes with the composition, and is given by

$$Q = \int dx \frac{dH}{dc} \frac{\partial c}{\partial t} \quad (3)$$

Using the approximation $\int_0^T D(T') dT' = \int_0^T D_0 \exp(-E/k_B T') dT' \approx \frac{k_B T^2}{E} D(T)$ [14], we arrive at (see Appendix):

$$\frac{T^2 Q(T)}{\beta} \approx \int dx \frac{T^2 D(T)}{\beta} f_1 \left[x, \frac{T^2 D(T)}{\beta} \right] f_2 \left[x, \frac{T^2 D(T)}{\beta} \right] = f \left[\frac{T^2 D(T)}{\beta} \right] \quad (4)$$

This equation states that the rescaled heat flow $\bar{Q} \equiv \frac{T^2 Q}{\beta}$ is a function only of the combined parameter $\frac{T^2 D(T)}{\beta}$. Thus, the peak temperatures T_m where \bar{Q} has reached a maximum is given by the following relationship

$$\ln \frac{\beta}{T_m^2} = A - \frac{E}{k_B T_m} \quad (5)$$

where A is a constant. In practice, the calorimetric peaks are usually sharp enough that T_m can be simply taken at maximum Q rather than at maximum \bar{Q} . Eq. (5) is identical in form to the Kissinger equation for chemical reaction kinetics, which has also been shown to be applicable to phase transformations occurring by nucleation and growth [15]. Eq. (5) therefore shows that the activation energy for diffusion in multilayer films can also be obtained using the Kissinger analysis, i.e., by plotting $\ln \frac{\beta}{T_m^2}$ vs. $\frac{1}{T_m}$, and obtaining the activation energy E from the slope $-\frac{E}{k_B}$. Although the activation energy for diffusion can be readily determined using this Kissinger-type analysis, determination of the pre-exponential term D_0 from the DSC traces is not trivial. One method is by forward modeling, i.e., by simulating the DSC curves and determining D_0 by minimizing the difference between simulated and measured peak temperatures. However, it is shown in the Appendix that under certain conditions, it is possible to estimate D_0 using simple expressions.

The above model implicitly assumes that the interdiffusion responsible for the heat flow signal is unidirectional, and hence the atom migration parallel to the surface of the multilayer thin films has to be negligible. The requirement of unidirectional diffusion is clearly satisfied in the regime of type A diffusion in which lattice diffusion dominates and the interfaces between adjacent layers are planar [16]. In the regime of type C diffusion in which the grain boundary diffusion dominates, although the interfaces are not planar, the diffusion is still unidirectional along the columnar grains that are commonly found in sputtered thin films [17]. For type B diffusion, the kinetics is more complicated since the concentration profile is controlled by both lattice and grain-boundary diffusion, and the model

here which employs only a single diffusivity is inadequate. Nevertheless, even in the regime of type B diffusion, the diffusivity derived here can still provide semi-quantitative information about the kinetics of diffusion.

Multilayer films of [Fe (25 nm)/Ni (25 nm)]₂₀ were prepared by DC magnetron sputtering from 99.95% Fe and 99.9% Ni elemental targets onto (100) Si substrates pre-coated with a 300 nm-thick Al layer. The base pressure of the sputtering chamber was better than 2×10^{-8} torr. The sputtering gas was ultrahigh-purity Ar at a pressure of 3 mTorr.

Following deposition, free-standing films were prepared by dissolving the Al layer in 10% NaOH solution. The released films were cleaned in distilled water, acetone and isopropyl alcohol and then dried in air. Approximately 10 mg samples of the multilayer were encapsulated in 99.95% Pt foil and examined using a Perkin-Elmer DSC-7 differential scanning calorimeter (DSC) at heating rates of 20, 40, 80 and 160 °C/min from 200 °C to 700 °C. XRD experiments for phase identification were conducted using a Scintag diffractometer with Cu K α radiation.

The XRD patterns of the Fe/Ni multilayer films are shown in Fig. 1. Peaks from both body-centered cubic (bcc) and face-centered cubic (fcc) structures are seen for the films in the as-deposited state. After annealing, only peaks from the fcc structure are observed. Thus, it is concluded that upon annealing, the layers interdiffuse and a fcc solid solution is formed.

The DSC traces of the Fe/Ni multilayer films are shown in Fig. 2. All curves show only a single exothermic peak resulting from the enthalpy change upon intermixing. The peak temperatures before and after the rescaling procedure detailed in the Theory section are listed in Table 1. The difference between the experimentally-measured peak temperature and the rescaled peak temperature was so small (<1 °C) that the rescaling procedure was neglected, and the experimentally-measured peak temperature was used for the determination of the activation energy.

The Kissinger plot is shown in Fig. 3. The activation energy for interdiffusion in the Fe/Ni multilayers is calculated from the slope of the plot as 1.6 ± 0.1 eV. The pre-exponential term D_0 is obtained by minimizing the difference in peak temperatures from the DSC experiments and the numerically-simulated traces. The peak temperatures of the simulated traces are listed in Table 1. For the simulations, the expression for the enthalpy of mixing is taken from [18].

Using this expression, the value obtained for $D_0 = 4 \times 10^{-3}$ cm²/s. It should be noted that the shape of the

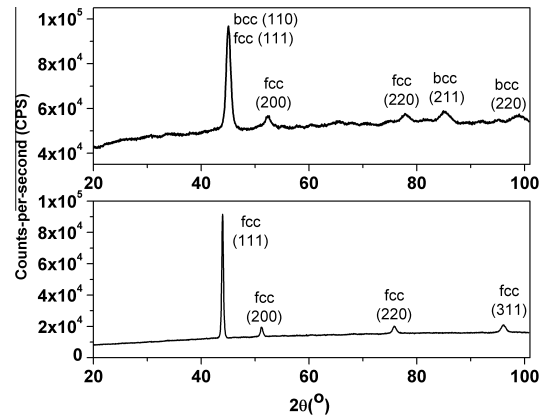


Fig. 1. XRD patterns of Fe–Ni multilayers before and after DSC experiments.

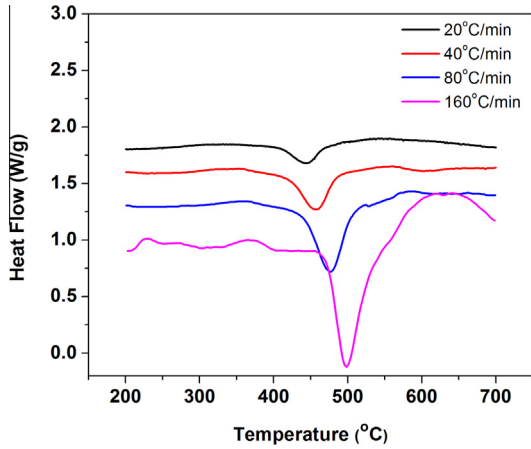


Fig. 2. DSC curves with different heating rates (endothermic up).

Table 1. Peak temperatures of DSC curves at different heating rates.

Heating rate (°C/min)	Peak (°C)	Rescaled peak (°C)	Simulated peak (°C)
20	443	443	438
40	457	458	456
80	477	477	474
160	498	496	492

numerically-simulated DSC traces could be different from experiment due to the fact that the instrumental thermal lag cannot be fully corrected; therefore the peak temperatures rather than full DSC traces were used in determining D_0 .

The derivation of Eq. (4) (see Appendix) relies on the implicit assumption that the diffusivity is independent of composition. The validity of this assumption can be examined using the reported lattice diffusivity in the Fe–Ni system [19], wherein $E = 3.34 \pm 0.05 \text{ eV}$ and D_0 varies within one order of magnitude from 10 at.% to 90 at.% Ni. The above expressions show only a weak composition dependence of diffusivity and activation energy.

The activation energy for lattice diffusion is a sum of the vacancy migration activation energy and the vacancy creation activation energy, and thus it is typically twice the activation energy for grain boundary diffusion. Grain boundaries act as ready sources or sinks for vacancies, thereby eliminating the vacancy formation energy barrier [20]. The effective activation energy for interdiffusion measured here is $1.6 \pm 0.1 \text{ eV}$, also half of the reported value for lattice diffusion at 3.2 eV [19]. Therefore, grain boundary diffusion is likely the diffusion mechanism in the Fe/Ni multilayers.

The diffusion mechanism in the Fe/Ni films can also be evaluated using reported values of the diffusivity. Fig. 4 plots diffusivities in the temperature range of 280–700 °C by extrapolation of high-temperature data to the temperature range of the current study [10,11,21–46]. Fig. 4 clearly shows that the diffusivity data split into two bands, with grain boundary diffusivities falling within the upper band and lattice diffusivities falling within the lower band. The effective diffusivity measured in the current study is closer and more parallel to the upper band representing grain boundary diffusion than to the lower band. Thus, it can again be concluded that the mechanism of diffusion in the Fe/Ni multilayers obtained here is grain boundary diffusion.

The above discussion can now be directed to the synthesis of L1_0 FeNi. In order to produce L1_0 FeNi from the

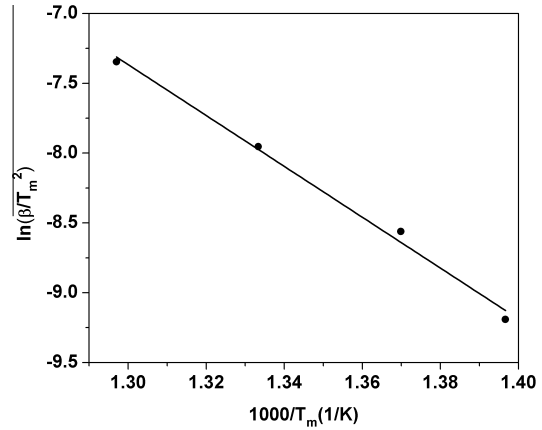


Fig. 3. Kissinger plot of peak temperatures. The slope is activation energy of diffusivity divided by Boltzmann's constant.

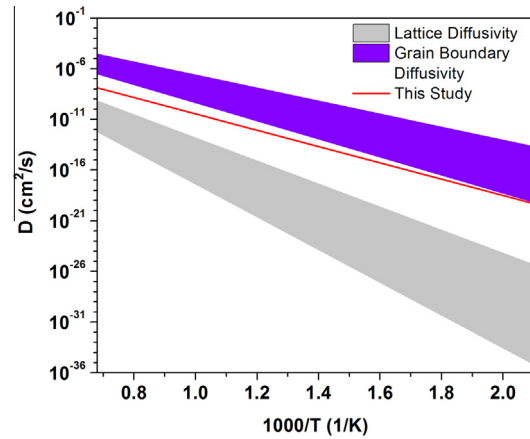


Fig. 4. Comparison between lattice diffusivity, grain boundary diffusivity and effective diffusivity in multilayer films studied here.

disordered matrix through isothermal annealing at a laboratory time scale, the diffusivity below 320 °C must be high enough to allow the phase transformation to proceed at a reasonable rate. The effective diffusivity in the Fe/Ni multilayer films is found to be more than five orders of magnitude higher than lattice diffusivity below the order–disorder temperature of 320 °C, and is comparable to that of Fe/Pt multilayers measured with X-ray reflectivity [47,48]. Previous reports show that in Fe films the A1 to L1_0 transformation is completed within hours at an annealing temperature of 300 °C [49]. Therefore, it can be concluded that diffusivity in ultrafine-grained FeNi alloys will not be the limiting factor for the formation of L1_0 FeNi. Rather, the formation of L1_0 FeNi will be constrained by the low driving force for the phase transformation. This is consistent with the conclusion of our study of diffusivity in multilayers with sub-10 nm periodicity using X-ray reflectivity [50].

Funding support under NSF CMMI-1111692 and 1259736 and under U.S. Department of Energy's Advanced Research Project Agency – Energy (ARPA-E) is gratefully acknowledged. The XRR experiments were carried out at the Center for Functional Nanomaterials, Brookhaven National Laboratory, which is supported by the U.S. Department of Energy, Office of Basic Energy Sciences, under Contract No. DE-AC02-98CH10886. A. Montes Arango is thanked for assistance with the DSC setup. L.H. Lewis, A. Montes Arango and N. Bordeaux are thanked for fruitful discussions.

In order to determine D_0 , it is necessary to include all experimental parameters in the derivation of Eq. (4)

$$c(x, T) \approx \sum_n (A_n \sin \frac{2\pi n}{L} x + B_n \cos \frac{2\pi n}{L} x) \times \exp \left(-\frac{4\pi^2 n^2 k_B}{L^2 E} \frac{T^2 D(T)}{\beta} \right) = c \left[\frac{x}{L}, \frac{T^2 D(T)}{\beta L^2 E} \right] \quad (\text{A.1})$$

$$\frac{\partial c(x, T)}{\partial t} \approx \sum_n (A_n \sin \frac{2\pi n}{L} x + B_n \cos \frac{2\pi n}{L} x) \frac{-4\pi^2 n^2}{L^2} D(T) \times \exp \left(-\frac{4\pi^2 n^2 k_B}{L^2 E} \frac{T^2 D(T)}{\beta} \right) = \frac{D(T)}{L^2} f_1 \left[\frac{x}{L}, \frac{T^2 D(T)}{\beta L^2 E} \right] \quad (\text{A.2})$$

$$\frac{\partial H}{\partial c} = \frac{\partial H}{\partial c}(c) \approx \frac{\partial H}{\partial c} \left(c \left[\frac{x}{L}, \frac{T^2 D(T)}{\beta L^2 E} \right] \right) = f_2 \left[\frac{x}{L}, \frac{T^2 D(T)}{\beta L^2 E} \right] \quad (\text{A.3})$$

$$Q = \int dx \frac{dH}{dc} \frac{\partial c}{\partial t} \approx \int d \frac{x}{L} \frac{D(T)}{L} f_1 \left[\frac{x}{L}, \frac{T^2 D(T)}{\beta L^2 E} \right] f_2 \left[\frac{x}{L}, \frac{T^2 D(T)}{\beta L^2 E} \right] \quad (\text{A.4})$$

$$\frac{QT^2}{\beta LE} = f \left(\frac{T^2 D}{\beta L^2 E} \right) \quad (\text{A.5})$$

The function f is determined by the thickness ratio of adjacent layers and the form of the enthalpy of mixing $H(c)$, and it is approximately universal for systems with a parabolic $H(c)$ (i.e. regular solutions) and equal thicknesses in all layers. The βLE term on the left side of Eq. (A.5) only affects the peak magnitude and not peak temperature, so this equation can be written as

$$\bar{Q} \equiv T^2 Q = f \left(\frac{T^2 D}{\beta L^2 E} \right) \quad (\text{A.6})$$

Therefore, for any binary thin-film multilayer satisfying the requirements that (1) all layers have equal thicknesses, (2) the DSC curves exhibit a single peak, (3) $H(c)$ is close to parabolic, then the following equation holds:

$$\frac{T_m^2}{\beta L^2 E} D(T_m) \approx M \quad (\text{A.7})$$

where T_m is the peak temperature at maximum \bar{Q} or approximately maximum Q . M is a universal constant, and $M = 16 \text{ K/J}$ determined using the values for the Fe–Ni system. This equation makes it possible to determine the pre-exponential term D_0 without the need to simulate the differential profile of the DSC curves.

- [1] L. Néel, J. Pauleve, R. Pauthenet, J. Laugier, D. Dautreppe, J. Appl. Phys. 35 (1964) 873.
- [2] J. Paulevé, A. Chamberod, K. Krebs, A. Bourret, J. Appl. Phys. 39 (1968) 989.
- [3] L.H. Lewis, F.E. Pinkerton, N. Bordeaux, A. Mubarak, E. Poirier, J.I. Goldstein, R. Skomski, K. Barmak, IEEE Magn. Lett. 5 (2014) 1.
- [4] K.B. Reuter, D.B. Willaims, J.I. Goldstein, Metall. Mater. Trans. 20A (1989) 711.
- [5] R.B. Scorzelli, Hyperfine Interact. 110 (1997) 143.
- [6] J. Pauleve, D. Dautreppe, J. Laugier, L. Néel, J. Phys. Radium 23 (1962) 841.

- [7] I.G. Kabanova, V.V. Sagaradze, N.V. Kataeva, Phys. Met. Metall. 112 (2011) 267.
- [8] A.L. Greer, F. Spaepen, in: L.L. Chang, B.C. Giessen (Eds.), Synthetic Modulated Structures, Academic, New York, 1985, p. 420.
- [9] A.F. Jankowski, Defect Diffus. Forum 266 (2007) 13.
- [10] T.J. Chuang, K. Wandelt, Surf. Sci. 81 (1979) 355.
- [11] D.C. Dean, J.I. Goldstein, Metall. Trans. A 17 (1986) 1131.
- [12] M. Vohra, M. Grapes, P. Swaminathan, T.P. Weihs, O.M. Knio, J. Appl. Phys. 110 (2011) 123521.
- [13] C. Michaelsen, K. Barmak, T.P. Weihs, J. Phys. D 30 (1997) 3167.
- [14] A.W. Coats, J.P. Redfern, Nature 201 (1964) 68.
- [15] H.E. Kissinger, Anal. Chem. 29 (1957) 1702.
- [16] L.G. Harrison, Trans. Faraday Soc. 57 (1961) 1191.
- [17] D. Gupta, P.S. Ho, Thin Solid Films 72 (1980) 399.
- [18] H. Okamoto, Phase Diagrams of Binary Iron Alloys, ASM International, Materials Park, 1993.
- [19] J.I. Goldstein, R.E. Hanneman, R.E. Ogilvie, Trans. Metall. Soc. AIME 233 (1965) 812.
- [20] R.W. Balluffi, J. Electron. Mater. 21 (1992) 527.
- [21] D.W. James, G.M. Leak, Philos. Mag. 12 (1965) 491.
- [22] A.R. Wazzan, J. Appl. Phys. 36 (1965) 3596.
- [23] J.S. Lee, B.H. Cha, Y.S. Kang, Adv. Eng. Mater. 7 (2005) 467.
- [24] S.V. Divinski, F. Hisker, Y.S. Kang, J.S. Lee, Chr. Herzig, Z. Metallk. 93 (2002) 256.
- [25] Y.S. Kang, J.S. Lee, S.V. Divinski, Chr. Herzig, Z. Metallk. 95 (2004) 76.
- [26] S.V. Divinski, F. Hisker, Y.S. Kang, J.S. Lee, Chr. Herzig, Interface Sci. 11 (2003) 67.
- [27] N.W. de Reça, C.A. Pampillo, Scr. Metall. 9 (1975) 1355.
- [28] D. Juve-Duc, D. Treheux, P. Guiraldeng, Mater. Sci. Eng. 42 (1980) 281.
- [29] H. Bakker, J. Backus, F. Waals, Phys. Stat. Sob. (b) 45 (1971) 633.
- [30] J.D. Tucker, R. Najafabadi, T.R. Allen, D. Morgan, J. Nucl. Mater. 405 (2010) 216.
- [31] G. Neumann, V. Tolle, C. Tuijn, Phys., B 363 (2005) 206.
- [32] W. Walsoe de Reça, C. Pampillo, Acta Metall. 15 (1967) 1263.
- [33] V. Ganesan, V. Seetharaman, V.S. Raghunathan, Mater. Lett. 2 (1984) 257.
- [34] J.R. MacEwan, J.U. MacEwan, L. Yaffe, Can. J. Chem. 37 (1959) 1629.
- [35] G.F. Hancock, G.M. Leak, Met. Sci. Technol. 1 (1967) 33.
- [36] K. Hirano, M. Cohen, B.L. Averbach, Acta Metall. 9 (1961) 440.
- [37] R.J. Borg, D.Y.F. Lai, Acta Metall. 11 (1963) 861.
- [38] B. Million, J. Ruzickova, J. Velisek, J. Vrestal, Mater. Sci. Eng. 50 (1981) 43.
- [39] T. Ustad, H. Sorum, Phys. Stat. Sol. (a) 20 (1973) 285.
- [40] A.D. Romig Jr., J.I. Goldstein, Metall. Trans. A 12A (1981) 243.
- [41] A.Ya. Shinyaev, Fiz. Metallov i Metallovedenie 6 (1958) 68.
- [42] A.Ya. Seinyaev, Izv. Akad. Nauk SSSR, Ser. fiz. 4 (1969) 182.
- [43] P. Guiraldeng, C.R. Acad. Sci. 264 (1962) 1994.
- [44] M. Badia, A. Vignes, Acta Metall. 17 (1969) 177.
- [45] H.A. Bakker, Phys. Stat. Sol. 28 (2) (1968) 569.
- [46] K. Maier, H. Mehrer, E. Lessmann, W. Schüle, Phys. Stat. Sol. 78 (2) (1976) 689.
- [47] V.R. Reddy, A. Gupta, A. Gome, W. Leitenberger, U. Pietsch, J. Phys.: Condens. Matter 18 (2009) 186002.
- [48] N. Zotov, J. Feydt, A. Savan, A. Ludwig, J. Appl. Phys. 100 (2006) 073517.
- [49] D.C. Berry, Ph.D. thesis, Carnegie Mellon University, Pittsburgh, 2007.
- [50] J. Liu, K. Barmak, J. Vac. Sci. Technol., A 33 (2015) 021510.